

SANDIA REPORT

SAND96-8596 • UC-413
Unlimited Release
Printed JUNE 1996

An Enhanced Search Methodology for Special Nuclear Materials

Scott Carichner

Prepared by
Sandia National Laboratories
Albuquerque, New Mexico 87185 and Livermore, California 94551
for the United States Department of Energy
under Contract DE-AC04-94AL85000

Approved for public release; distribution is unlimited.



Issued by Sandia National Laboratories, operated for the United States Department of Energy by Sandia Corporation.

NOTICE: This report was prepared as an account of work sponsored by an agency of the United States Government. Neither the United States Government nor any agency thereof, nor any of their employees, nor any of the contractors, subcontractors, or their employees, makes any warranty, express or implied, or assumes any legal liability or responsibility for the accuracy, completeness, or usefulness of any information, apparatus, product, or process disclosed, or represents that its use would not infringe privately owned rights. Reference herein to any specific commercial product, process, or service by trade name, trademark, manufacturer, or otherwise, does not necessarily constitute or imply its endorsement, recommendation, or favoring by the United States Government, any agency thereof or any of their contractors or subcontractors. The views and opinions expressed herein do not necessarily state or reflect those of the United States Government, any agency thereof or any of their contractors or subcontractors.

SAND96-8596
Unlimited Release
Printed June 1996

An Enhanced Search Methodology for Special Nuclear Materials

Scott Carichner
Exploratory Systems
Sandia National Laboratories/California

ABSTRACT

This report is an overview of the first phase of work done to use data fusion to improve the search process for weaponizable radioactive materials. Various methods were examined to provide a system-level optimization to the problem. Data fusion signal-processing techniques using sensor counts and sensor position information with reasonable computation time showed an initial four-fold improvement in the overall search system performance compared to optimal processing without knowledge of sensor position. With the inclusion of data visualization techniques, a centralized search controller has access to information that improves the main search parameters: range, search time, and search confidence. The improvement is significant enough to justify the next phase of work which includes: adding neutron sensor data, investigating the position location system, and further tests and refinements of the system.

CONTENTS

	PAGE
I. Background.....	7
II. Enhanced Search System.....	7
System Goals.....	7
System Description.....	8
System Performance Drivers.....	8
III. Sensor Data Fusion.....	9
Potential of Data Fusion.....	9
Physical Model.....	9
Background Filtering.....	11
Model Fitting.....	12
Data Display and Interpretation.....	13
IV. Experimental Results.....	14
Experimental Technique.....	14
Data.....	15
Visualization Results.....	16
V. Conclusions.....	18
VI. Figures.....	21

AN ENHANCED SEARCH METHODOLOGY FOR SPECIAL NUCLEAR MATERIALS

I. Background

Over a year ago, Sandia's Exploratory Systems Center completed a study to identify promising areas of research to counteract the increasing threat of unconventional nuclear attacks – concluding that there were several areas Sandia should pursue further. This report describes initial work done in using sensor data fusion techniques to enhance the ability to search for weaponizable radioactive materials.

During the formative stages of this project it was determined that the focus would be on a system that improved the capability to conduct a search when intelligence information has identified a localized area that may contain radioactive materials in a weapon or the component materials for such a weapon. It is widely recognized that past research in detectors and signal-processing algorithms has led to very capable DOE search equipment. Our goal was to identify how to centrally process *all* the available information from existing equipment and operations to optimize important search metrics such as range, search time, and confidence in the results. Finally, we wanted to display the data in a manner that would allow a central operator to control the search.

II. Enhanced Search Systems

System Goals

The search system must be rapidly deployable to buildings such as office buildings, factories, warehouses, residences, etc. A team searches the building using the gamma radiation signature emitted from SNM (special nuclear materials). A central command post collects data from each searcher, processes it and then an operator interprets the data. The operator decides how to continue the search depending on his confidence that a source has been identified or that the absence of a source has been verified. Depending on the intelligence reports concerning the building, a confidence level will be set to trigger the searcher's advance to the next building on the list. It is assumed that the central controller can guide the search on a periodic basis by communicating an updated set of instructions to the searchers after each "round" of search is completed. It is also assumed that the central site has no real technical information on the building (such as floor plans or construction material). The search strategy is optimized without such knowledge and any extra information, such as floor plans or maps, will be used to improve the interpretation of the output of the enhanced search system.

System Description

The proposed enhanced search system uses several team members to carry the gamma sensors and data transmission systems through the building. During this process the integrated gamma sensor counts are transmitted to three receivers that are deployed around the building. (See Figure 1) A proposed spread spectrum system that works similar to the global positioning system not only senses the searcher's position but transmits the gamma counts measured on the same frequency band. A central system takes the three receiver measurements, calculates a position for each searcher and logs the gamma readings.

The central processing site runs a sensor fusion algorithm (described in Section 3) that will optimally combine the information from each searcher at each point in time to give a graphic representation of the gamma sources in the building along with the confidence associated with those points. From this data, the central operator makes decisions regarding the best way to proceed with the search by either moving on to the next target building or by searching specific areas more thoroughly.

The sensor fusion algorithm is run with batches of search data in near real-time. The operator can make search decisions after each of these batches of data are processed.

System Performance Drivers

During the planning of the enhanced search project several technical means to improve the system performance were investigated to ensure that we had a fundamental understanding of the relative importance of each subsystem. In the planning we looked at improvements to the sensor that would permit more accurate determination of the gamma photon energy. These were not pursued because unless the active collection area of the device was similar to the current sensors the improvements were counterbalanced by the loss in total counts and subsequent increase in noise. Only small marginal improvements seemed possible with this technique.

It was discovered that often the limiting factor in searching for a gamma source was the repeatable variation in the building's gamma background. These variations in the background were repeatable because they were caused by the geometry and construction materials of the building. Any reduction in statistical noise associated with further improvements to the current sensor had no effect on this background variation – a fact that is accounted for in the data fusion algorithm described in Section 3. Without knowledge of the building materials and detailed floor plans, these background variations must be considered random noise.

However, by collecting all the available gamma signal information and adding position labels to the data, the data can be fused together to extract information that is statistically more meaningful. This method provides improvements to the important system metrics. All other system parameters have remained the same, including the searcher's walking speed, the sensor and the search path.

III. Sensor Data Fusion

Potential of Data Fusion

Radioactive decay is accurately modeled by a Poisson counting process. One of the properties of this process is that counts made on non-overlapping time periods are independent. In this context this means that each data measurement made by each searcher is independent of the time period they were taken as long as the statistical parameters are constant during the time period. This assumption has shown to be valid for the short time period that the search is conducted. Thus neither the order in which the measurement is taken, or which of the searchers took the measurement is important. All that really matters is *where* the measurement was taken. Adjacent measurements in space are *not* independent. A nearby source of gamma photons, whether it is a target or background, point-source or diffuse-source, will make the measurements made in that region correlated. Data fusion is a method for taking all these noisy measurements and processing them to make a better estimate of the system parameters than could otherwise be done with only the data from independently operated sensors.

Physical Model

The method we are using for data fusion relies upon a physical model of the system. This model has components that are developed from first principles and others that have been experimentally identified and parameterized. The model starts with a 2-dimensional field that represents the area being searched. This scalar field has a gamma amplitude associated with each (x,y) spatial index into the field. The gamma amplitude represents the sum of all target and background photons between 50 and 500 keV as would be measured if an omni-directional sensor was placed at point (x,y) in the field. The 2-dimensional field is parallel to the floor of a building and is displaced approximately three feet above the floor.

In the model the gamma amplitude is a zero-mean random variable consisting of the sum of three random variables. The gamma amplitude is zero-mean because

a gross estimate of the background that is clearly not due to a target point source is subtracted from the raw data. The source of the three random variables are:

- B , the integration of photons from nearby distributed background sources such as concrete pillars, cement floors
- N , the statistical variation that occurs in any Poisson counting process and
- S , the result of a nearby point source target (if it exists).

The background count rate, B , is too complex to predict based on the limited information the searcher has regarding the building architecture and construction. In buildings with large masses of concrete, B is the biggest source of fluctuation with current sensor equipment. In lightweight buildings such as trailers, the fluctuation in B is several times less than N . The background, B , is modeled as an independent Gaussian process at each point in the scalar field for simplicity, even though it is correlated at nearby points. The mean is zero due to the removal of the gross estimated background from all the data. The standard deviation of the background data, B , is calculated from the data sample itself assuming that each data sample is uncorrelated.

The noise, N , is the statistical fluctuation associated with the Poisson counting process. The mean of N is zero and the standard variation is equal to the square root of the total raw data count prior to background subtraction. The standard deviation is nearly constant due to the fact that the background level is large compared to the values of B and S . For example, the mean of the raw data may change from 150 to 200 counts per second but the standard deviation, σ_N , will only change from 12 to 14 counts.

The signal, S , is the component from a target of interest. A nearby point source will contribute to the count rate according to the formula

$$H = \frac{C}{d^2} \cdot e^{-\lambda d} \quad (1)$$

where: C is a constant relating the counts for a specific detector at 1 foot per curie of radiation, d is the distance from the source to the point in the field, and λ is an empirically derived constant representing the average shielding factor of buildings. The formula indicates why the counts due to the source fall off quickly with distance.

A serious simplification regarding the shielding between the source and the detector is made in eq. 1. In a vacuum the first term represents the $1/d^2$ reduction effect that any point source of energy has with distance. However, any intervening mass will reduce the received count further by scattering photons away from the detector or absorbing the photon altogether. Without knowledge of the intervening mass

between the source and sensor it has turned out to be adequate to model the shielding as if it were a homogeneous cloud of shielding material everywhere in space. This effect is modeled by the $e^{-\lambda d}$ term in eq. 1. The constant, λ , is empirically picked to halve the signal every 10 feet. The exponential term dominates the $1/r^2$ term at distances greater than tens' of feet since it falls off much quicker. Experiments described in Section 4 have shown that this is the simplest model that is accurate enough for this application. Our attempts at using the model without the shielding were unsatisfactory. Some generic knowledge about the building may be used to pick λ in a more-refined model. A structure made from light building materials should in general have a smaller λ . Structures with large open interior spaces should also have smaller λ .

Background Filtering

As previously mentioned it is necessary to subtract out an estimate of the global background contribution since the signals of interest are small variations on this background bias. Any signal that is comparable to the background is so strong that it is a trivial exercise to detect it.

An algorithm was developed that enables irregularly spaced raw data from multiple searchers and multiple passes in the same area to be averaged together in a weighted manner. A 2-dimensional surface is created that represents the weighted average of the raw data. The weighting is proportional to the inverse of the distance from the data point. Once this surface is created it is spatially filtered in two dimensions by taking the 2-dimensional discrete cosine transform and low-pass filtering in the spatial frequency domain. After taking the inverse transform, a slowly undulating approximation to the background is all that is left (see Figure 2). This surface is sampled at the original data points to create a background estimate for each raw data point (the white trace in Figure 3) which is subsequently subtracted from the raw signal (the yellow trace in Figure 3).

It is important that subtraction of the background estimate does not remove potential target response from the raw data. By restricting the background estimate to low spatial frequencies the only target that would be subtracted out would be a very distant target that was not seen at any closer point during the rest of the search. This is unlikely as the search has to be arranged so that the detector passes all points in the building within its maximum range in order to confidently assess the building.

Model Fitting

Searching for a target in the random data field has been turned into a problem of model fitting. A point-wise algorithm takes each point, (x,y) , in the field, and fits a point-source model to the data. The result of this fitting operation is a best-fit amplitude for the source and a measure of how much error exists between the data and model. The tricky part of this problem has been finding a good way to decide what the best-fit point source is and how good the fit is compared to the fluctuations in fit that occur even when no point-source target is in the field.

The algorithm starts by creating a matched filter for the (x,y) point under consideration. This is done by creating a matrix, h , with components,

$$h_{i,x,y} = \frac{1}{d_{i,x,y}^2} \cdot e^{-\lambda d_{i,x,y}} \quad (2)$$

where
$$d_{i,x,y} = \sqrt{(x_i - x)^2 + (y_i - y)^2}, \quad (3)$$

(x_i, y_i) are the coordinates of the i^{th} point in the measurement vector, and (x,y) is the point in the random field being tested. The index variable i ranges from 1 to M , the number of sensor data points.

For a given (x,y) , the matched-filter matrix represents the normalized expected value of the S - component of the raw data. It uses the distance to each data measurement point and the physical model from eq. 1. Since $h_{i,x,y}$ is normalized the actual contribution in counts per second to the data measurement requires a scaling constant, $C_{x,y}$, to be found according to the amplitude of the point-source at (x,y) .

The amplitude constant, $C_{x,y}$, can be found with a weighted least mean squares fitting algorithm. The data points must be weighted because the nearby data points have a higher signal-to-noise ratio and therefore they are more "important" in estimating the value of $C_{x,y}$. It can be shown that the optimum weighting for each data point is proportional to the value of h_i . This makes sense intuitively since the amplitude of the point-source falls off as h_i but the noise ($B_i + N_i$) remains constant. The error function for the weighted least mean squares is

$$\epsilon_{x,y} = \frac{1}{\sum_j W_{j,x,y}} \cdot \left[\sum_i W_{i,x,y} (h_{i,x,y} - Y_i)^2 \right] \quad (4)$$

where Y_i is the zero-mean raw data vector and the weighting factor is $W_{i,x,y} = C_{x,y} \cdot h_{i,x,y}$. By taking the derivative of this function, $\frac{\partial \epsilon_{x,y}}{\partial C_{x,y}}$, and setting it to zero, a $C_{x,y}$ can be found that minimizes this error function. This is referred to as the best-fit amplitude source at that particular (x,y) in the random field.

Another matrix, pf , is needed to qualify the values in the amplitude matrix C . The better the data fits (i.e. the smaller the error, $\epsilon_{x,y}$) the more confident we can be that the result is due to a point-source at (x,y) and not due to a confounding noise and/or background effect. The simplest metric is the matrix of errors ϵ . Unfortunately, it is difficult to compare the meaning of different errors at different (x,y) . It is better to calculate the theoretical standard deviation of the distribution of the random variable $C_{x,y}$ assuming that there is no target point-source in the field. Then the normalized function, $pf_{x,y} = \frac{C_{x,y}}{\sigma_{x,y}}$, indicates the likelihood of the fluctuation. A $pf_{x,y}$

value of +3 would indicate that the value of $C_{x,y}$ is 3 standard deviations greater than the expected value. The likelihood that $C_{x,y}$ falls three standard deviations from the mean due to background alone can be derived from the Gaussian error function. The formula for $\sigma_{x,y}$ was derived using the adequate approximation that all the Y_i are independent. The following formula for $\sigma_{x,y}$ was derived by calculating the expected value of the square of $C_{x,y}$ with no sources in the area.

$$\sigma_{x,y}^2 = E[C_{x,y}^2] = \frac{\sigma_Y^2 \cdot \sum_i h_{i,x,y}^4}{\left[\sum_i h_{i,x,y}^3 \right]^2} \quad (5)$$

σ_Y^2 is a constant for each data set and it is calculated using the data in Y . The C and pf matrices, the two outputs of the data fusion algorithm, are used to search the field for sources and to display the data in a graphical form.

Data Display and Interpretation

Data visualization relies on the fact that complex information can be understood quickly and efficiently if it is presented in the correct manner. The information that has been calculated from the raw data vector is contained in two, 2-dimensional matrices. The first (see Figure 4) is the matrix C . (We used a one foot grid for calculation but sometimes the data is plotted on a 1 or 2 foot grid for readability.) The second (see Figure 5) is the matrix pf . Note that in each figure there is no data (holes) at the sensor sample points. In the calculations as distance goes to zero at these points the models break down. These plots ignore the sensor sample points.

Since there are two, 2-dimensional matrices to interpret it was necessary to find a way to display the data graphically. Either matrix itself provides incomplete information. After experimenting with many methods our solution (see Figure 6) was to plot a surface where for each point, (x,y) , the height of the surface is proportional to the size of the source, C , and the color of the surface is the number of standard deviations, pf , above or below the mean of the background distribution.

When evaluating the combined data plot (Figure 6) the first things to notice are areas of high source amplitude. By examining the color, the likelihood of a real point source can be determined. High amplitude areas with deviations within three standard deviations are not very meaningful nor are low amplitude areas near the path even with greater than three standard deviations. The most likely point sources show up as peaked amplitudes with standard deviations above three.

Due to edge effects the best fit amplitude sometimes becomes quite large as the distance from a sample point increases. The only real problem the edge effects cause is that their high amplitude can tend to scale the graph so that more interesting reasonable amplitudes are no longer visible on the surface.

The operator that interprets this data has a lot of information at their disposal to make judgments on the validity of a source. Things like the surrounding area, point in the building, distance to the path, size of the source, likeliness of the reading, shape of the peak, are all information that can provide cues for further decision making. It is hoped, but not yet established, that the operator will learn from experience how to extract extra information from this view of the data output similar to the way submarine sonar operators do. As is always true of human versus computer decision-making comparisons, the human has certain advantages and disadvantages. The human can process in parallel very subtle information cues and make decisions regarding those clues that are difficult to program into an automated algorithm. The computer can meticulously scan all the data and interpret it to identical criteria. We feel that the combination of the computerized algorithm to process and display the data along with the human's interpretation of the visual data is an excellent combination to take advantage of both of the strengths of each.

IV. Experimental Results

Experimental Technique

In order to develop and test the algorithm described in the preceding sections a simple test system was developed to gather data. The equipment is shown in Figure 7a. A large sodium iodide (NaI) scintillator detector was used along with a multi-channel analyzer (MCA) to generate an energy histogram for each one second integration period. The entire histogram was stored for each data point on a notebook computer, but, when the data was transferred to a desktop computer for post-processing it was integrated from 50 keV to 500 keV to obtain a single scalar number of counts for each data point. The system diagram of the hardware is in Figure 7b.

For experiments a ^{133}Ba source was set in the middle of the lab (see Figure 8) and a cart was wheeled through nearby hallways (see Figures 9a and 9b) collecting data at

4 foot intervals. A computer program integrated the data for one second and logged the data and position information to a file. There was little need for accuracy in traveling 4 feet between samples. The results were unchanged if the position was off by several feet because the hallway created a constrained rectilinear path that prevented the position error from constantly accumulating. Usually floor tiles or carpet patterns were sufficient to mark off the distance. The computer program accepted input regarding whether each step was left, right or straight, in order to maintain relative position information from the origin of the measurements.

After a test run was conducted (usually on a 90 foot by 32 foot rectangle) the data was transferred to a desktop computer for processing. The processing was done in Matlab (a commercial computation and visualization software package) running on a Macintosh. The algorithms have not been optimized yet, but the prototype versions in Matlab run in less than two minutes. This value indicates that the algorithms are simple and robust enough to work in near real-time with some modifications. The Matlab system permits easy data plotting as well as allowing processing on UNIX, MS Windows, or the Macintosh operating system.

Data

A large number of experiments were run to generate the current algorithms. During the course of gathering data the results were compared to a standard reference platform, the DOE detection system, in order to benchmark this technique. Data was taken in three different Sandia buildings to compare the effects of different styles of buildings on the performance.

Data was taken with and without target sources to establish a baseline. The background is usually the limiting factor of the detection process and therefore an important piece of information. In one building with concrete floors, concrete pillars, and large laboratories – the background fluctuations, B , were greater than the statistical fluctuations, N . Since the statistical noise did not contribute much, the results are nearly the same each time data is taken over the same path. In this case, extra data is of limited value if it comes from an (x,y) where measurements were already taken. The fact that walking slower (integrating longer) or walking the same path two or more times is sometimes of little help in reducing the background fluctuation is a non-intuitive result. The repeatable background fluctuations mask the weak signals regardless of measurement time. If a source is present and improvements are attempted by increasing the integration time, the source and background increase at the same rate and therefore the detection probability does not change. However, by adding data points at new (x,y) there can be further reinforcement of a point source signal and reduction in distributed background sources. This occurs because the point source continues to fit the point source model better and better while the distributed source fits poorly with the physical model.

In some instances the background fluctuation, B , is not larger than the statistical fluctuation, N , and then improvements *can* be obtained by counting longer at the same points. This improvement will continue until the statistical fluctuation has been driven below the level of background spatial fluctuation. This is more typical in buildings that are homogeneous or made from low-background construction material. A lightweight modular building at Sandia showed these characteristics.

An interesting effect observed in our mapping of building backgrounds was the large increases that were seen in the background near a stairwell and an elevator in one of the buildings. These large changes are not subtracted out by the background estimation algorithm and subsequently if the detector is walked past these objects in a single straight-line path it is hard to distinguish the results from a large source. But, if the path is convoluted in that area so as to obtain new spatial sample points, the distributed background source does not fit well with the point source model. Therefore, the identification of this background anomaly as a point source target is less likely than it would be without fusion of the position information. The reason for the background increases in these areas was not investigated, but, others had already warned us of the problem and suggested that it was either due to the increase of exposed concrete building materials or cosmic radiation.

In each experiment with a simulated source, ^{133}Ba was used. This isotope of Barium is easy to obtain and work with, while having its major gamma output at an energy similar to Plutonium (^{239}Pu). At first, small 10 μCi sources were used to examine the algorithm. If there was shielding (doors, walls, equipment, etc.) this was too small to detect in our geometry. A larger 3 mCi source of ^{133}Ba was obtained. With this source it was possible to sheath it with circular rings of lead sheet to vary the output so that a large range of signal source strengths could be tried in the same exact geometry. This made it easy to make comparisons between the different responses to each of the strengths. Although background measurements were made at several sites, the source experiments were all done in the same lab because of safety restrictions involving the source.

Visualization Results

The following data illustrates the output of the algorithm and the data visualization routines. Other sets of data that are not shown have similar characteristics.

The following dataset was taken in the building shown in Figures 8, 9a, and 9b, but other experiments in different locations have indicated that the results are not biased by this particular location. A plot in Figure 10 shows for this test set-up the outline of the external walls of the building and the numbered sample data points. The sample point positions are the same for the rest of the datasets.

Looking back to Figure 3, it depicts two concepts that are important aspects of the data fusion algorithm. First, the raw data and background estimates along the path are shown. The background estimate was determined by creating an average surface from the raw data, low-pass filtering it to retain the slowly varying estimate, and then by re-sampling it at the same points as the original data. This graph demonstrates with experimental data that the background varies slower than the contribution from a point source. This justifies the filter parameters used for background estimation.

Second, Figure 3 shows how the matched filter model fitting works in actual practice. The matched-filter in the figure was chosen to be at the specific coordinates where the ^{133}Ba point source was placed. It is displayed after scaling by the constant $C_{37,15}$. This waveform has the minimum error defined by eq. 4. The areas where the amplitude of the matched-filter deviates the most from background were weighted most heavily to generate the best-fit. Because the path comes within range of the source at two different points this matched filter has two areas that it weighs heavily.

Figure 11 is an output plot of the type discussed in Section 3.5 for the lab with no point source in the area. Figure 11 is on the same scale as Figure 6 and 12 for direct comparisons. Notice that there are small changes in the surface height that (if enlarged to greater Z-axis scale) would look like a very small point-source. These are caused by the random fluctuations of the background, B , and noise, N , components of the raw data. The color of the peaks show that they are not good fits to the data. In fact they are well within ± 3 standard deviations, exactly where you would expect the signal to be for a random field with no sources. The most extreme points occur near $(x,y)=(10,10)$. A good fit has been found to a very small source near the path, but an operator can dismiss this point because the source is too small to be of interest at a range from the search path of only several feet.

Figure 12 is the same experiment with a medium strength source at the point $(x,y) = (37,15)$. Notice that the source appears as both the largest amplitude source in the region and a good fit, in that it is over 4 standard deviations above the mean. This source is large enough to obscure most of the background fluctuations that were in Figure 11. However, this comparison could not be done in field-use since there would not be any known background-only plot with which to compare.

There is nothing special about where the source was placed in this experiment except that it is not too near to the sample path such that the data point weighting would only look at a few adjacent points. There was ample and random shielding materials between the source and detector along the entire path, including but not limited to: metal/plasterboard walls, metal cabinets, fume hoods, equipment racks, closed doors and heavy chemistry lab countertops.

Figure 6 is the same experiment with a weak source (the source has been stopped down with lead sheet shielding to the near limit of sensitivity). Further reduction of the source amplitude would force the fit function to be in an area that could be mistaken for background fluctuation when the interpreter does not have prior background information. The effective source size at this point is a factor of four times smaller than the minimum strength of source detectable by the reference platform that we used for comparison. Figure 12 was taken with the weakest detectable source in the reference platform.

It should be noted that the size of the source once detected can be used to determine whether to pursue investigation of this source and the location can be used to plan further surveillance of that area.

V. Conclusions

This project has provided a strong indication that a data fusion technique can improve the search for special nuclear material in the scenario described in the report. This improvement appears to be significant enough to warrant a study to see if this system can be engineered into a field deployable unit for search. In comparisons against the same sensor in current equipment, with the same search parameters, this data fusion method detected a source with four times weaker amplitude. We were careful to not bias this comparison – the test area was typical of several buildings we studied during the course of the project and the shielding was random. As a side benefit, this data fusion concept can shift the burden of expertise to the central controller in scenarios where trained searchers are not practical or available. The independence of the measurement to the time it was taken could allow searching to be done in parallel with building occupant's normal tasks.

As with any experiment some simplifications have been made to test the feasibility. The computational complexity of the current algorithm scales well as the search area increases. As the algorithm takes a couple of minutes to process on a desktop Macintosh computer we are confident that it will run fast enough for an operational situation. Since we have integrated all the energy counts in a large window the system can look for a broad range of radioactive materials without degradation in performance.

Continuation of this work would investigate the fusion of neutron measurements into the system. The algorithm supports this addition whether the neutron detectors are in the same platform as the gamma detector or separate units carried by separate searchers. The most promising aspect of adding the neutron detectors is that the background signal for neutrons comes from an independent phenomena from the gamma background. This would indicate that the inclusion of this data will enhance

the confidence from any neutron-emitting point source while decreasing the viability of a distributed gamma background source that randomly appears as a possible point source. Another promising aspect of neutron detection in the system is that shielding materials that tend to reduce the gamma signal (high Z materials) are not as effective in reducing the neutron signals, while low Z materials that have little effect on the gamma signal do reduce the neutron signal. This indicates that the fusion of the two types of data could have a large payoff and that random shielding that occurs from intervening material between the detector and the source would tend to be negated.

But there are still one main issue that would need further work before fielding a prototype system. A brief initial feasibility study showed that the RF position determining system described in the system concept would be a simple and elegant solution to the problem, but engineering difficulties associated with RF propagation in this environment make it a non-trivial task to field the system. Other potential methods may have to be investigated including inertial systems and landmark referencing systems.

6 Figures

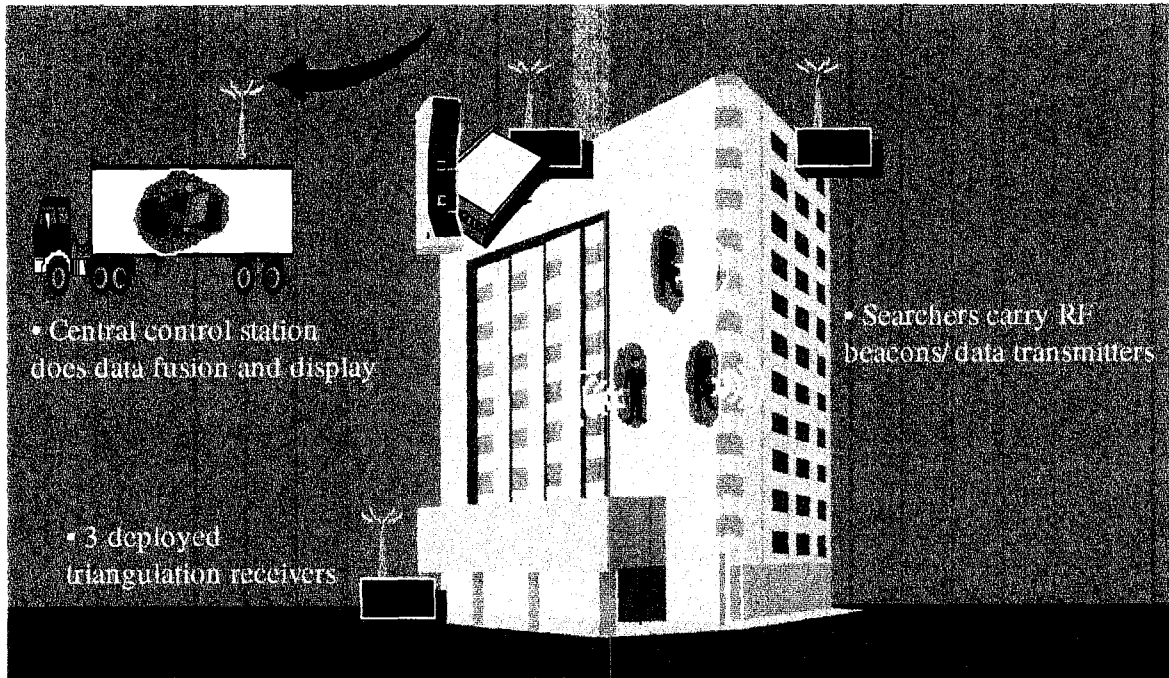


Figure 1 Enhanced search system concept showing multiple searchers transmitting the sensor signal, three triangulation receivers to locate the position of the transmission, and a central control station running the data fusion algorithm.

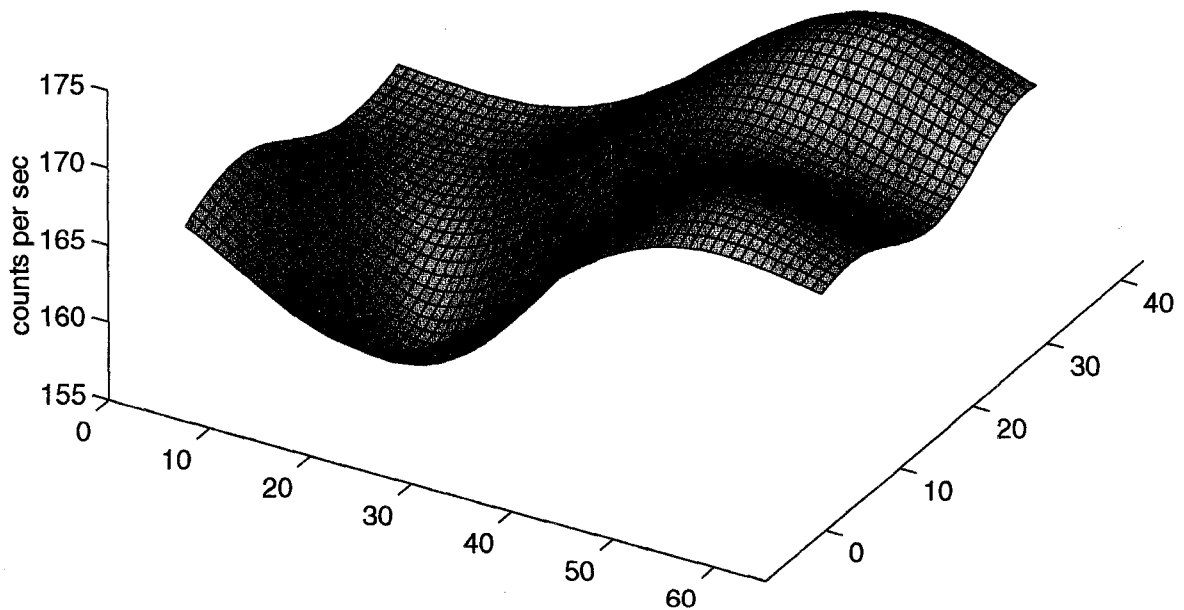


Figure 2 This is the background estimate after spatial low-pass filtering. It is subtracted from the raw data after re-sampling along the sensor path.

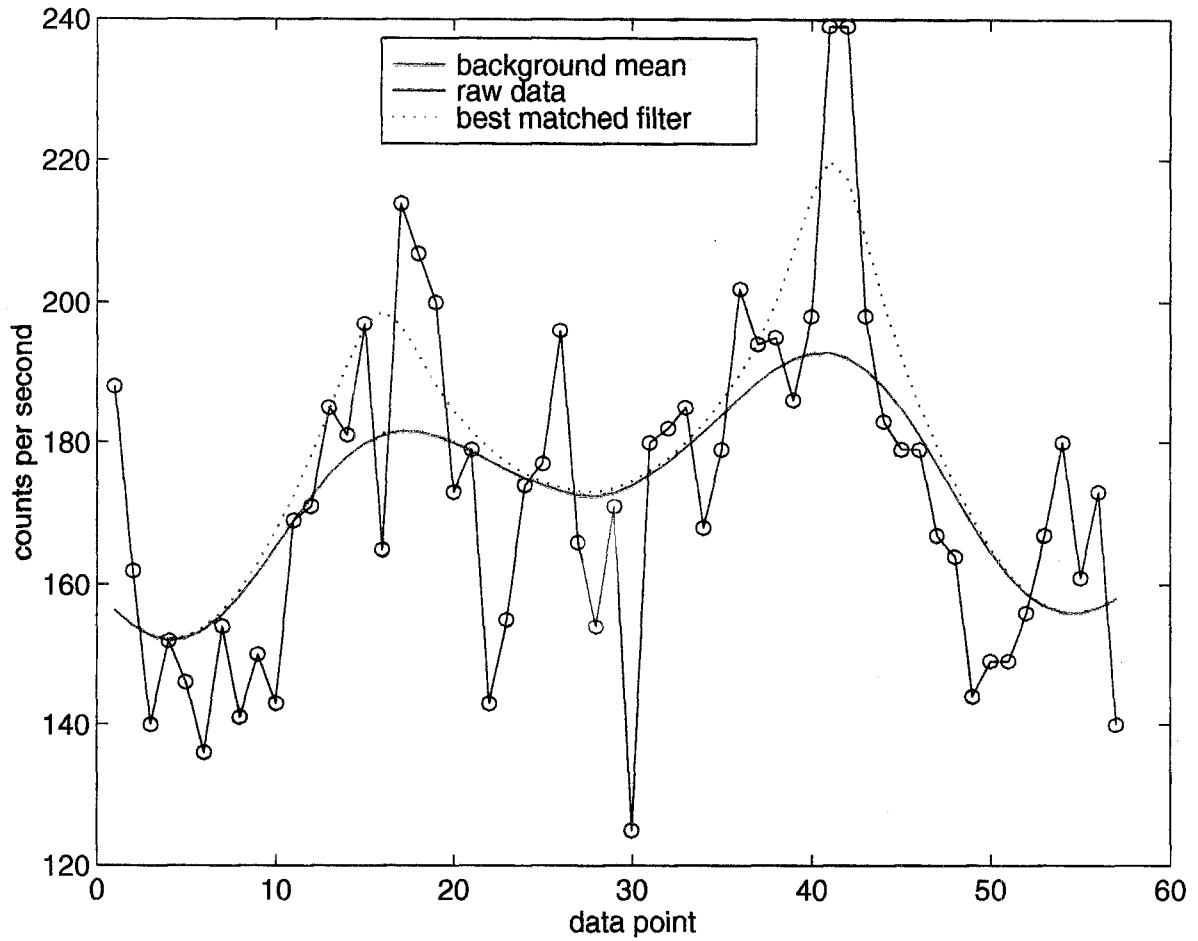


Figure 3 Raw data, background estimate and best-fit matched-filter. In this dataset the displayed matched-filter is calculated for the actual known source location. The amplitude of the matched-filter is the best weighted least-mean-squares fit to the raw data.

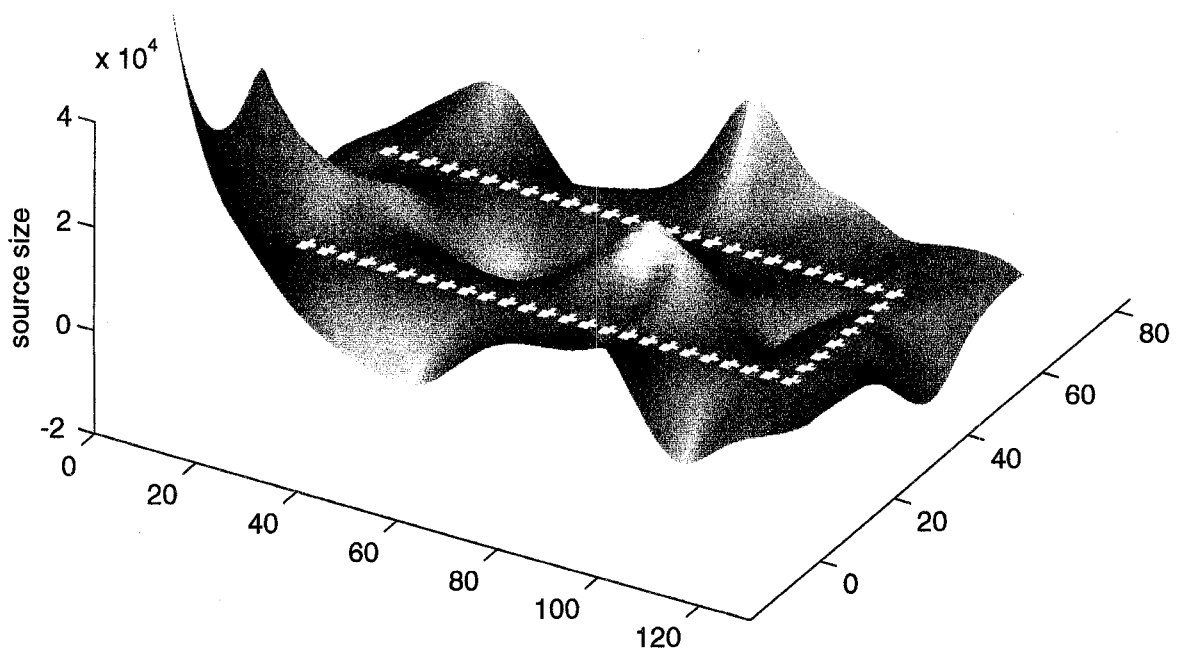


Figure 4 Best-fit amplitude source matrix with a source at (74,30). The holes show the sensor path.

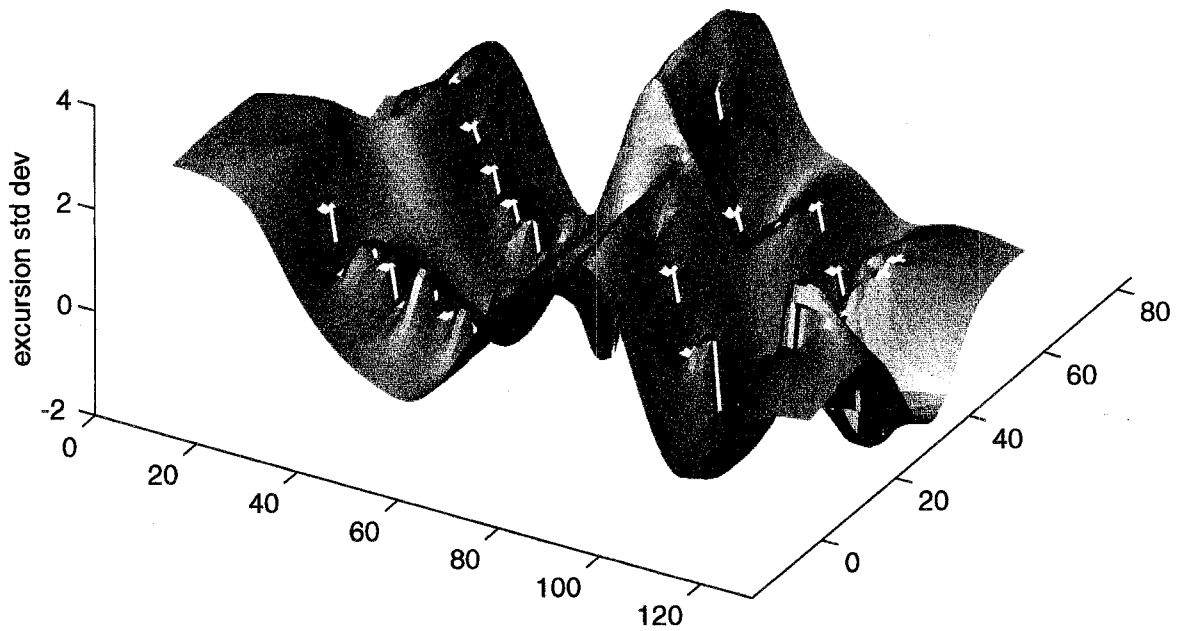


Figure 5 Best-fit source size in units of standard deviation from the mean background. The standard deviations are calculated from the sensor data assuming it is only background (which is a good approximation for most of the sensor path).

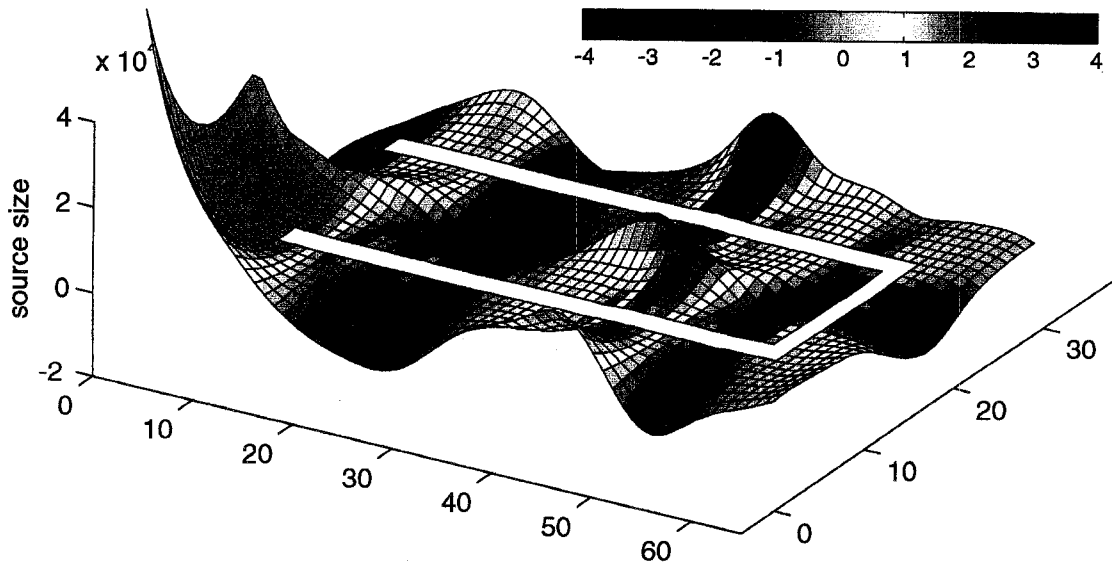


Figure 6 Joint size and likelihood plot from experimental data with a weak source at (37,15).

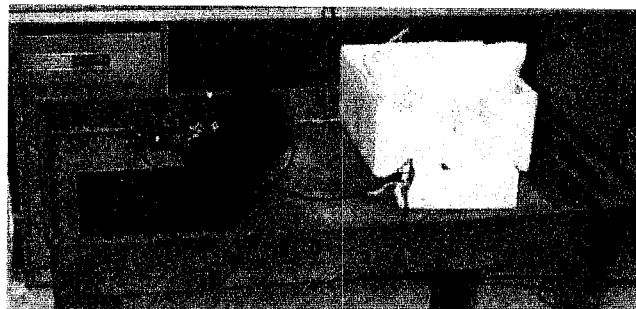


Figure 7a Experimental hardware. A large scintillator detector and preamp are connected to a multi-channel analyzer. Data is saved on a portable computer.

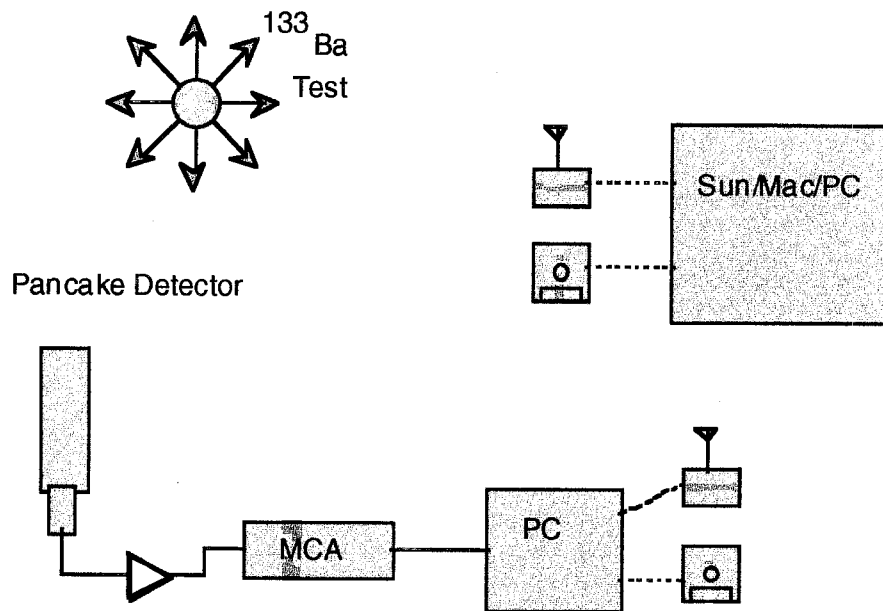


Figure 7b Block Diagram of Experimental Hardware. The data is transferred by disk or RF modem.

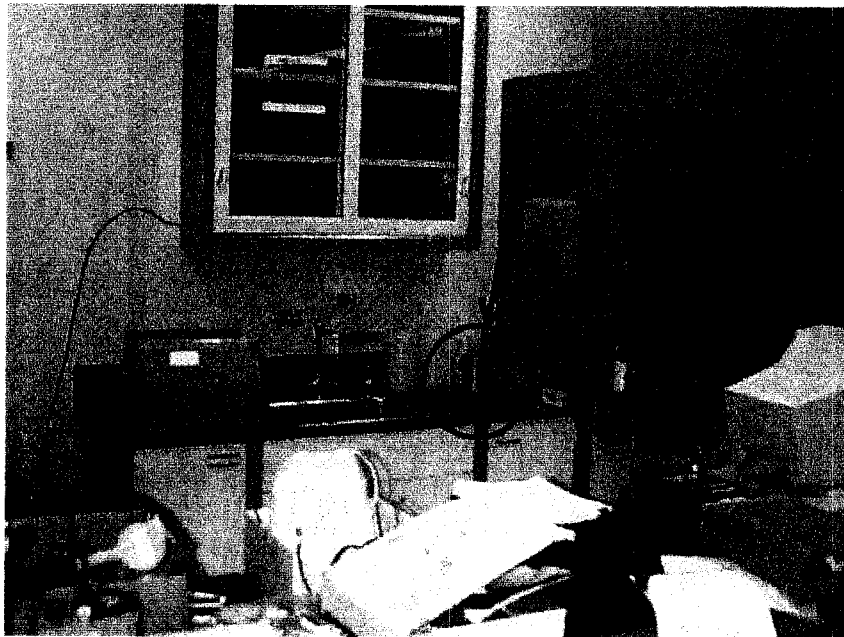


Figure 8 The Barium source location is highlighted. The source is near the center of the two hallways but otherwise was put in a typical location in the room.



Figure 9a Typical section of hallway surrounding laboratory showing the path of the sensor and the large amounts of shielding material in the hallway.

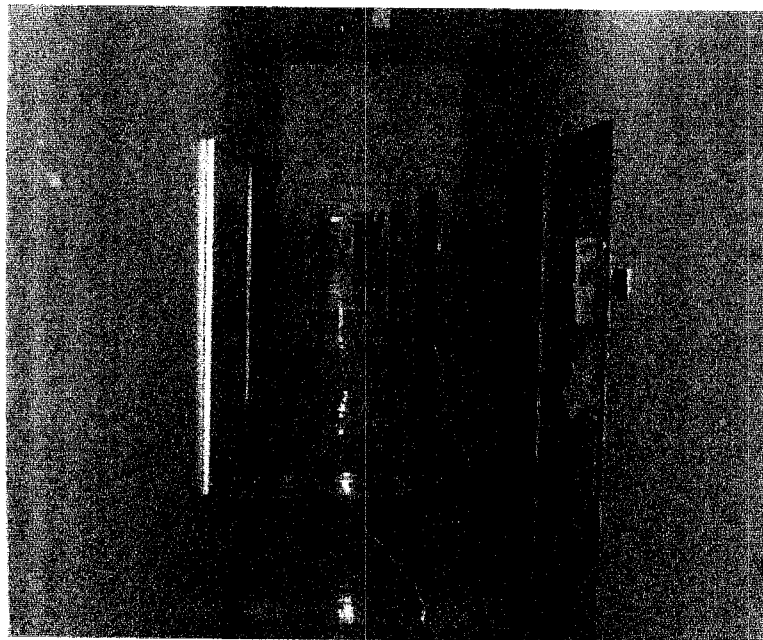


Figure 9b The hallway on the opposite side of the building contained less variation in the shielding material.

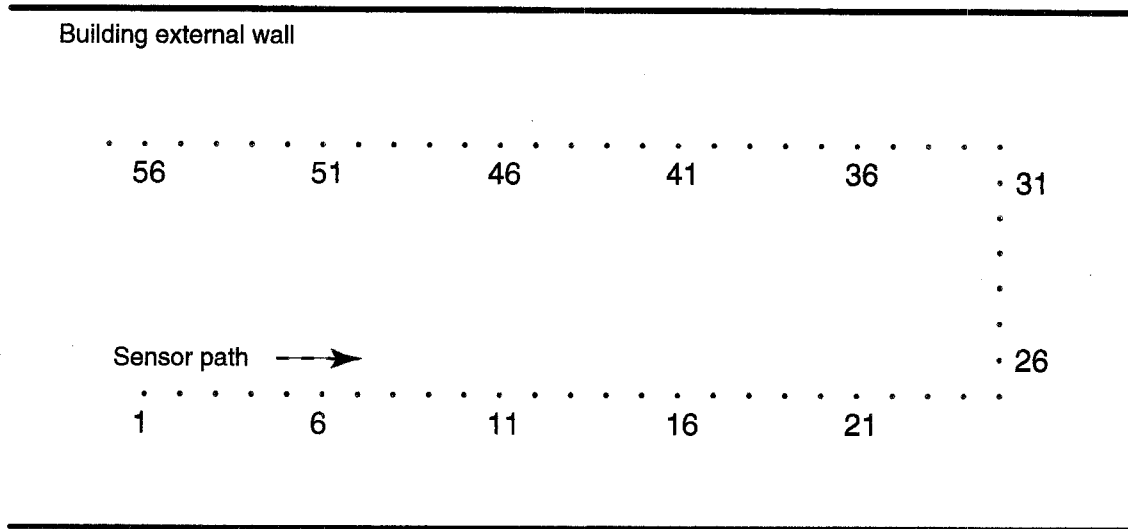


Figure 10 The other source plots are all based on this sensor path and building geometry. Each data sample is numbered and displayed in Figure 3.

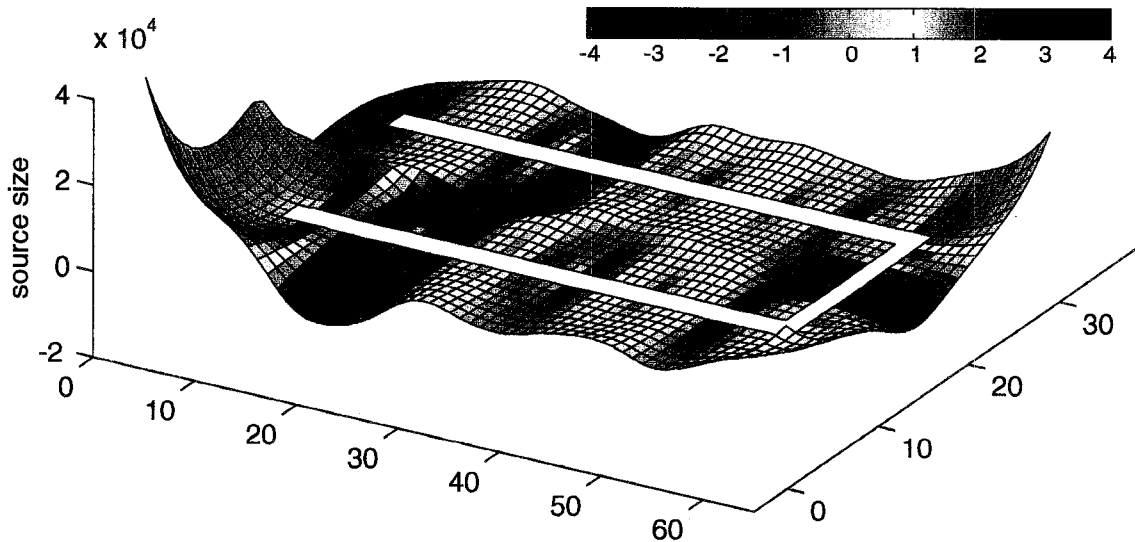


Figure 11 Joint size and likelihood plot from experimental data with a no source. The fluctuations are due to the spatial variance of the background.

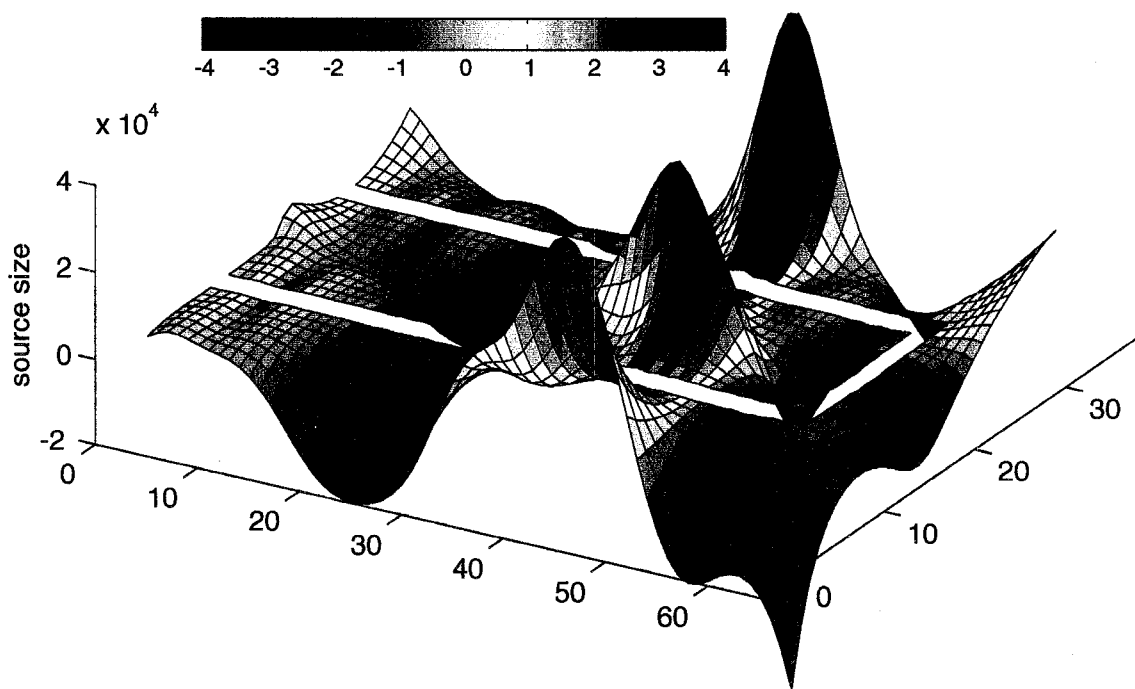


Figure 12 Joint size and likelihood plot from experimental data with a medium strength source at (37,15).

UNLIMITED RELEASE

INITIAL DISTRIBUTION:

Tom Dahlstrom
Bechtel Nevada
PO Box 98521, M/S RSL-21
Las Vegas, NV 89193-8521

MS 0469 John M. Taylor, 5006
MS 0761 L. M. Ford, 5822
MS 9001 T. O. Hunter, 8000

Attn: M. B. Wright, 2000
E. E. Ives, 5200
W. J. McLean, 8300
R. C. Wayne, 8400
P.N. Smith, 8500
L. A. West, 8600
T. M. Dyer, 8700
P. Brewer, 8800
D. L. Crawford, 8900

MS 9004 M. E. John, 8100
MS 9103 Tim Berg, 8111
MS 9103 Scott Carichner, 8111 (10)
MS 9103 Don Sheaffer, 8111
MS 9103 Greg Thomas, 8111 (3)
MS 9201 Michael Johnson, 8114
MS 9409 Ralph James, 8250
MS 9214 Philip Kegelmeyer, 8117
MS 9409 Jim Lund, 8250
MS 9409 Jeff Markakis, 8250
MS 9409 Richard Olsen, 8250
MS 9402 Arlyn Antolak, 8715
MS 0449 David Jeppeson, 9403
MS 0427 Ron Trelue, 9403
MS 0763 Rodney Wilson, 9614
MS 0767 Lewis Newby, 9602
MS9021 Technical Communications Department, 8815
For OSTI (10)
MS9021 Technical Communications Department, 8815/
Technical Library, 4414, MS 0899
MS0899 Technical Library, 4414, (4), MS 9018
Central Technical Files, 8940-2 (3)